

Modeling of Multitype Particle Flow Using the Kinetic Theory Approach

Hadjira Iddir and Hamid Arastoopour

Dept. of Chemical and Environmental Engineering, Illinois Institute of Technology, Chicago, IL 60616

DOI 10.1002/aic.10429

Published online April 21, 2005 in Wiley InterScience (www.interscience.wiley.com).

The effects of particle size and/or density on particle interaction and overall behavior of granular flow were studied using the kinetic theory approach. The kinetic theory for granular flow was extended to mixtures of multitype particles assuming a non-Maxwellian velocity distribution and energy non-equipartition. Each type of particles was considered as a separate phase with different velocity and granular temperature. The resulting momentum equation for each particulate phase includes phase interaction arising from collisional pressure and particle–particle drag force. When applied to simple shear granular flow of a binary mixture, this model predicts well the energy non-equipartition and the stresses of particulate systems with different sizes and densities. © 2005 American Institute of Chemical Engineers AICHE J, 51: 1620–1632, 2005

Keywords: kinetic theory, particle collision, granular mixture, granular shear flow, energy non-equipartition

Introduction

Granular flows exhibit complex behavior arising from the co-existence of two different behaviors within the flow: solid-like and fluid-like behaviors. Collisions of particles of different mechanical properties and corresponding fluctuations that occur during flow make the system more complicated. In this work, we investigate the effect of particle mechanical properties (size, particle density) on granular flow behavior using the kinetic theory approach.

Originally the kinetic theory was developed by Chapman and Cowling¹ for gases to predict the behavior of mass point molecules whose interaction energies are conserved. Nearly two decades ago, this theory was extended to particulate flow where the interactions between particles are not conserved. Savage and Jeffrey² were probably the first to apply the kinetic theory to rapidly deforming material in the form of smooth hard spherical particles (ideal mixture). In their derivation, to calculate the stress tensor arising from interparticle collisions, they assumed that the collisions between particles were purely elastic. Although in some granular flows the restitution coef-

ficient is restrained to values close to unity, its deviation from unity results in a significant variation in the properties of granular flow. This was shown first by Jenkins and Savage.³ They extended the kinetic theory of an idealized granular mixture to predict the rapid deformation of granular material by including energy dissipation during collision for nearly inelastic particles. Later on, based on the original work of Savage and Jeffrey² and Jenkins and Savage,³ Lun et al.⁴ developed a theory that predicts the simple shear flow behavior for a wide range of restitution coefficients. Many models for granular flow were then developed based on the kinetic theory approach.^{5–7}

All the above-cited works assumed mixtures of identical density and size. However, real systems are composed of particles of different properties, in which segregation by size or density may occur during the flow, as was shown by Arastoopour et al.⁸ In their work, they developed a hydrodynamic model for a mixture of gas and a multisize solid phase. They applied it to simulate one-dimensional flow in a vertical pneumatic conveying line. They showed that the particle size has a substantial effect on the pressure drop and choking velocity and particles segregate along the vertical transport line. The experiment of Savage and Sayed⁹ showed the stresses in a shear cell, for a monosize mixture of polystyrene beads, were about five times higher than those for a binary mixture.

Correspondence concerning this article should be addressed to H. Arastoopour at chearastoo@minna.iit.edu.

Jenkins and Mancini¹⁰ extended the kinetic theory of dense gases to a binary mixture of idealized granular material for the low dissipation case. Consequently, they assumed that the energy dissipation in the collision is sufficiently small, such that the deviation of the temperature of each component from the mixture granular temperature is very small. Thus, in the application of their model, they assumed energy equipartition. Based on the work of Jenkins and Mancini,¹¹ Arnarson and Willits^{12,13} extended the kinetic theory to a binary mixture using the Chapman and Enskog procedure. They solved the Boltzmann's equation near the steady-state equilibrium assuming energy equipartition and almost equal particle mass to calculate the transport coefficients. They found that the shear viscosity was three times higher than that obtained using only Maxwellian velocity distribution. In 2002 Alam et al.¹⁴ generalized the model of Willits and Arnarson¹³ to a mixture of particles having different mass and size. However, their model was limited to energy non-equipartition. Zamankhan¹⁵ solved the kinetic equation using the Grad method and assumed that the particles fluctuate with the same energy; he concluded that energy non-equipartition must be included in mixtures with different particle properties. Garzó and Dufty¹⁶ showed theoretically that energy non-equipartition was violated for inelastic collisions of particles of different mechanical properties. This was experimentally confirmed by Wildman and Parker¹⁷ and Feitosa and Menon.¹⁸ Their experimental results showed the coexistence of two granular temperatures when the binary mixture was exposed to external vibrations. Huilin et al.^{19,20} used the work of Manger²¹ to develop a model for two-size particles with different granular temperatures; however, in the approach they used—by taking the arithmetic average of the particles' properties in the collisional operator—the momentum source vanishes. Thus, they had to include an additional momentum source in their governing equations without clear explanation. Furthermore, their integration of the constitutive equations was inappropriate, thus making their model limited to only the energy equipartition case. This is evident from their results of frequency of collisions ($N_{ik} \neq N_{ki}$), and the nonsymmetrical expression of the collisional pressure tensor.

Recently, Garzó and Dufty²² solved the kinetic equation for systems away from equilibrium; thus, their model could capture not only the energy non-equipartition, but also the flow behavior for a broader range of restitution coefficients. However, their model is restricted to dilute systems, where the radial distribution function was close to unity.

In this work, the kinetic theory is extended to a multitype (size and/or density) mixture, assuming a non-Maxwellian velocity distribution and energy non-equipartition. Each group type is represented by a phase, with an average velocity and a fluctuating energy or granular temperature. Unlike previously cited publications, where the fluctuations of the flow variables are about the mixture average, we assumed that each type of particles was considered by a phase, which means that the interaction between the phases is at the interface. In our approach, the deviation from the Maxwellian velocity distribution is in each individual particulate phase. In this case Maxwellian velocity distribution was assumed at the interface. This also resulted in manageable equations and made the mathematical derivation of the model possible. Then we solved the Boltzmann's equation for each particulate phase using the Chap-

man-Enskog procedure by adding a perturbation to the Maxwellian velocity distribution function.^{1,23}

Herein we begin by developing a model that represents a multiphase mixture consisting of particles of different sizes and densities interacting through collisions.

Our model was applied to simulate a simple shear flow and compared to the theory of Jenkins and Mancini¹⁰ with non-equipartition assumption, as well as to the molecular dynamics (MD) simulation of Galvin et al.²⁴

Model Development

The present model was obtained by considering a mixture of N solid phases (N is the number of solid phases); each phase is composed of smooth inelastic hard spheres. The assumption of hard spheres suggests that the collisions are almost instantaneous, so that binary collisions may safely be assumed. Each particulate phase i contains particles of mass m_i and diameter d_i that collide with each other in phase i . The collisions between particle i and other particles of different phases occur at the interface between phase i and other particulate phases. Each particle in phase i moving with instantaneous velocity \vec{c}_i is subject to an external force $\vec{F}_{i,ext}$. At any time t the probable number of particles per unit of volume $d\vec{r}$, with velocity varying between \vec{c}_i and $\vec{c}_i + d\vec{c}_i$, is the product of the single velocity distribution function $f_i^1(\vec{c}_i, \vec{r}, t)$ and the variation of the velocity $d\vec{c}_i$

$$n_i(\vec{r}, t) = \int f_i^1(\vec{c}_i, \vec{r}, t) d\vec{c}_i \quad (1)$$

Thus, the mean value of any property of phase i , $\psi_i(\vec{c}_i)$, is defined as

$$\langle \psi_i \rangle = \frac{1}{n_i} \int \psi_i(\vec{c}_i) f_i^1(\vec{c}_i, \vec{r}, t) d\vec{c}_i \quad (2)$$

The rate of change of the mean value of any property ψ_i in a fixed element of volume $d\vec{r}$ is attributed to the effect of the external force, the collisional rate of production (arising from all possible collisions with all the particles in the mixture), and the net influx of the property ψ_i . In this context, the equation of change for the particle property of phase i may be expressed as

$$\sum_{p=1}^N \langle (\psi_{ci})|_p \rangle = \frac{\partial}{\partial t} (n_i \langle \psi_i \rangle) + \nabla \cdot (n_i \langle \psi_i \vec{c}_i \rangle) - \frac{n_i}{m_i} \left\langle \vec{F}_{i,ext} \cdot \frac{\partial \psi_i}{\partial \vec{c}_i} \right\rangle \quad (3)$$

where $\sum_{p=1}^N (\psi_{ci})|_p$ is defined as the difference between the postcollisional and the precollisional properties of particle i arising from all possible collisions with all the particles in the mixture. The collision of particle i with other particles in the same phase results in the constitutive relation for each phase, and the interaction of phase i with other phases results in interfacial forces between particulate phases. The average of $\sum_{p=1}^N (\psi_{ci})|_p$ is defined as

$$\sum_{p=1}^N \langle (\psi_{ci})|_p \rangle = \sum_{p=1}^N \langle \psi'_i - \psi_i \rangle|_p = \sum_{p=1}^N \iiint \int (\psi'_i - \psi_i) f_{ip}^2(\vec{r}_i, \vec{c}_i; \vec{r}_p, \vec{c}_p) d\vec{k}_{ip} d\vec{c}_i d\vec{c}_p \quad (4)$$

For impending collisions, the integrals in Eq. 4 must be carried out only for values of $\vec{c}_{ip} \cdot \vec{k}_{ip} > 0$.

The complete pair distribution function $f_{ip}^2 = f_{ip}^2(\vec{c}_i, \vec{r}_i; \vec{c}_p, \vec{r}_p)$ is defined as the probability of finding, at time t , two particles i and p such that they are centered on \vec{r}_i and \vec{r}_p , and having velocities within the range $\vec{c}_i, \vec{c}_i + d\vec{c}_i$ and $\vec{c}_p, \vec{c}_p + d\vec{c}_p$.

Following Jenkins and Savage,³ the assumption of chaos along with the consideration of the correlation function allows us to write the pair distribution function as the product of the single velocity distributions, f_i^1 and f_p^1 , weighted by the spatial pair-distribution function at contact, $g_{ip}(\varepsilon_i, \varepsilon_p)$

$$f_{ip}^2\left(\vec{c}_i, \vec{r} - \frac{d_{ip}}{2} \vec{k}; \vec{c}_p, \vec{r} + \frac{d_{ip}}{2}\right) = g_{ip}(\varepsilon_i, \varepsilon_p) \cdot f_i^1\left(\vec{c}_i, \vec{r} - \frac{d_{ip}}{2} \vec{k}\right) \cdot f_p^1\left(\vec{c}_p, \vec{r} + \frac{d_{ip}}{2}\right) \quad (5)$$

where $\vec{c}_{ip} = \vec{c}_i - \vec{c}_p$ is the relative instantaneous velocity and $d_{ip} = (d_i + d_p)/2$.

\vec{k}_{ip} is the unit vector connecting the centers of the two particles, located at \vec{r}_i and \vec{r}_p , respectively, and directed from i to p . In the remaining text, we consider $\vec{k}_{ip} = \vec{k}$.

The collisional rate of production per unit of volume, $\sum_{p=1}^N \langle (\psi'_i - \psi_i) \rangle|_p$, was evaluated by Jenkins and Mancini¹⁰ as a sum of a symmetric (γ_{cip}) and antisymmetric (χ_{cip}) terms

$$\sum_{p=1}^N \langle \psi'_i - \psi_i \rangle|_p = \sum_{p=1}^N (-\nabla \cdot \chi_{cip} + \gamma_{cip}) \quad (6)$$

where

$$\chi_{cip} = -\frac{d_{ip}^3}{2} \iiint \int (\psi'_i - \psi_i) f_{ip}^2\left(\vec{c}_i, \vec{r} - \frac{d_{ip}}{2} \vec{k}; \vec{c}_p, \vec{r} + \frac{d_{ip}}{2}\right) \times \vec{k}(\vec{c}_{ip} \cdot \vec{k}) d\vec{k} d\vec{c}_i d\vec{c}_p \quad (7)$$

$$\gamma_{cip} = d_{ip}^2 \iiint \int (\psi'_i - \psi_i) f_{ip}^2\left(\vec{c}_i, \vec{r} - \frac{d_{ip}}{2} \vec{k}; \vec{c}_p, \vec{r} + \frac{d_{ip}}{2}\right) \times (\vec{c}_{ip} \cdot \vec{k}) d\vec{k} d\vec{c}_i d\vec{c}_p \quad (8)$$

Here χ_{cip} and γ_{cip} are the collisional fluxes and sources, respectively.

Substituting Eqs. 7 and 8 into the equation of change (Eq. 4) the continuity, momentum, and fluctuating energy equations were obtained for ψ_i equal to m_i , $m_i \vec{c}_i$, and $1/2(m_i C_i^2)$, respectively.

Continuity equation

The continuity equation for the solid phase i may be written as

$$\frac{\partial \varepsilon_i \rho_i}{\partial t} + \nabla \cdot (\varepsilon_i \rho_i \vec{v}_i) = 0 \quad (9)$$

where $\varepsilon_i \rho_i = n_i m_i$ is the phase i density, ε_i is its solid volume fraction, and ρ_i is its material density. Here $\vec{v}_i = \langle \vec{c}_i \rangle$ is the mean velocity of the particle i . The instantaneous velocity \vec{c}_i is defined as the sum of the average velocity \vec{v}_i and peculiar velocity \vec{C}_i : $\vec{c}_i = \vec{v}_i + \vec{C}_i$ with $\langle \vec{C}_i \rangle = 0$.

Momentum equation

The momentum equation for phase i may be expressed as

$$\varepsilon_i \rho_i \frac{D}{Dt} (\vec{v}_i) + \nabla \cdot \left(\sum_{p=1}^N \bar{P}_{cip} + \bar{P}_{ki} \right) - \frac{\varepsilon_i \rho_i}{m_i} \vec{F}_{iext} = \sum_{p=1}^N \vec{F}_{Dip} \quad (10)$$

where the material derivative is

$$\frac{D}{Dt} () \quad (11)$$

the kinetic pressure tensor is

$$\bar{P}_{ki} = \rho_i \varepsilon_i \langle \vec{C}_i \vec{C}_i \rangle \quad (12)$$

the collisional pressure tensor is

$$\bar{P}_{cip} = \chi_{cip} (m_i \vec{c}_i) \quad (13)$$

and the collisional momentum source is

$$\vec{F}_{Dip} = \gamma_{cip} (m_i \vec{c}_i) \quad (14)$$

Fluctuating energy equation

The fluctuating energy equation for solid phase i may be expressed as

$$\begin{aligned} \frac{3}{2} \frac{\varepsilon_i \rho_i}{m_i} \frac{D \theta_i}{Dt} + \nabla \cdot \left(\vec{q}_{ki} + \sum_{p=1}^N \vec{q}_{cip} \right) - \left(\bar{P}_{ki} + \sum_{p=1}^N \bar{P}_{cip} \right) : \nabla \vec{v}_i \\ = \sum_{p=1}^N (N_{ip} - \vec{v}_i \cdot \vec{F}_{Dip}) \end{aligned} \quad (15)$$

where

$$\theta_i = \frac{1}{3} m_i \langle \vec{C}_i \cdot \vec{C}_i \rangle \quad (16)$$

where θ_i is the granular temperature or the fluctuating granular energy of the solid phase i . The kinetic heat flux is

$$\vec{q}_{ki} = \rho_i \varepsilon_i \langle \vec{C}_i C_i^2 \rangle \quad (17)$$

the collisional energy flux is

$$\vec{q}_{cip} = \chi_{cip} (m_i c_i^2) \quad (18)$$

and the collisional energy dissipation is

$$N_{ip} = \gamma_{cip} (m_i c_i^2) \quad (19)$$

In the above governing equations, the relevant variables describing the flow field are the average velocities, the solid volume fractions, and the granular temperatures evaluated at location \vec{r} of the center of the particle at time t .

Kinetic equation

The kinetic equation that characterizes the flow of multiphase system are as follows

$$\left(\frac{\partial}{\partial t} + \vec{c} \cdot \nabla + \frac{\vec{F}_{iext}}{m_i} \cdot \nabla_{\vec{c}} \right) f_i^l = \sum_{p=1}^N \frac{d_{ip}^2}{4} \iint [g_{ip}(\vec{r}, \vec{r} + \vec{k}d_{ip}/2) f_i^l(\vec{c}_{i1}, \vec{r}, t) f_i^l(\vec{c}_{i2}, \vec{r} + \vec{k}d_{ip}/2, t) - g_{ip}(\vec{r}, \vec{r} - \vec{k}d_{ip}/2) f_p^l(\vec{c}_{p1}, \vec{r}, t) f_p^l(\vec{c}_{p2}, \vec{r} + \vec{k}d_{ip}/2, t)] \times (\vec{c}_{ip} \cdot \vec{k}) d\vec{c}_p d\vec{k} \quad (20)$$

where $g_{ip}(\vec{r})$ is the spatial pair-distribution function when the particles i and p are in contact. A solution of Eq. 20 near the equilibrium was obtained using the Chapman–Enskog method^{1,23}

$$f_i^l = f_i^0 (1 + \phi_i) \quad (21)$$

where f_i^0 is the Maxwellian velocity distribution

$$f_i^0 = n_i \left(\frac{m_i}{2\pi\theta_i} \right)^{3/2} \exp \left[-\frac{m_i C_i^2}{2\theta_i} \right] \quad (22)$$

where ϕ_i , a perturbation to the Maxwellian velocity distribution, is a linear function of the first derivative of n_i , θ_i , and \vec{v}_i . Note that ϕ_i is function of the phase mean velocity \vec{v}_i , and not the total flow velocity because, as mentioned earlier in the introduction, each kind of particles is treated as a separate phase and the interaction is at the interface.

The objective of this work is to describe the hydrodynamic behavior of a dense granular mixture where energy non-equipartition is taken into account. We assumed that each type of particles is a phase, the interaction between the phases is at the interface, and the deviation from the Maxwellian velocity distribution is in each individual particulate phase. As will be shown in the next section, our theoretical results agreed qualitatively well with the available experimental results and quantitatively with the MD simulation.

In a similar analysis, Willits and Arnarson¹³ solved the

Boltzmann's equation based on the Maxwellian reference state and the revised Enskog equation. Although the range of applicability of the present effort and the work of Willits and Arnarson is the same, the major differences between the two studies are non-equipartition and unequal particle size properties considered in our model. Willits and Arnarson assumed a multicomponent mixture where all the particles fluctuate about the same mass average velocity and having the same granular temperature. In our work, we considered a multiphase granular flow where each phase is represented by particles having separate properties, velocities, and granular temperatures.

Let us turn our attention, for a while, to the function $g_{ip}(\varepsilon_i, \varepsilon_p)$ that describes a multisize mixture of hard spheres at contact. Lebowitz²⁵ proposed a function that is the generalization of the Percus–Yevick equation for a mixture of hard spheres. This function was determined theoretically for a fluid of an N -component mixture. It takes into account two effects: a direct effect of particle i on particle p , and an indirect effect in which particle i influences all other particles. Following is the Lebowitz expression for $g_{ip}(\varepsilon_i, \varepsilon_p)$.

$$g_{ip}(\varepsilon_i, \varepsilon_p) = \frac{[d_p g_{ii}(\varepsilon_i, \varepsilon_p) + d_i g_{pp}(\varepsilon_i, \varepsilon_p)]}{2d_{ip}} \quad (23)$$

where

$$g_{ii}(\varepsilon_i, \varepsilon_p) = \frac{1}{1 - \varepsilon_i - \varepsilon_p} + \frac{3d_i}{2(1 - \varepsilon_i - \varepsilon_p)^2} \sum_{p=1}^N \frac{\varepsilon_p}{d_p} \quad (24)$$

At high solid volume fraction, the radial distribution function proposed by Lebowitz diverges from the Alder and Wainwright²⁶ MD simulation results. The MD simulation results show a reasonable limiting value for the radial distribution when ε approaches the single-phase maximum packing, ε_{\max} . We believe the results from MD simulation are more general; therefore we modified the Lebowitz radial distribution function such that it agrees with the results from the Alder and Wainwright MD simulation at both lower and higher solid volume fractions. The proposed function, which is used in our calculations, may be written as

$$g_{ii}(\varepsilon_i, \varepsilon_p) = \frac{1}{[1 - (\varepsilon_i + \varepsilon_p)/\varepsilon_{\max}]} + \frac{3d_i}{2} \sum_{p=1}^N \frac{\varepsilon_p}{d_p} \quad (25)$$

The expression of $g_{pp}(\varepsilon_i, \varepsilon_p)$ is obtained by simply interchanging the indices i and p .

Figure 1 shows a good agreement between the proposed radial distribution functions and the Alder and Wainwright MD simulation results.

The constitutive relations for kinetic and collisional pressures, heat fluxes, collisional momentum, and energy dissipation are derived and shown in the Appendix.

Before applying our model along with the constitutive relations to any flow system, we should identify the number of terms in the expressions of R_0 to R_{10} needed to accurately predict the flow behavior. We used Wildman and Parker¹⁷ granular energy data for a binary mixture in vibrofluidized bed.

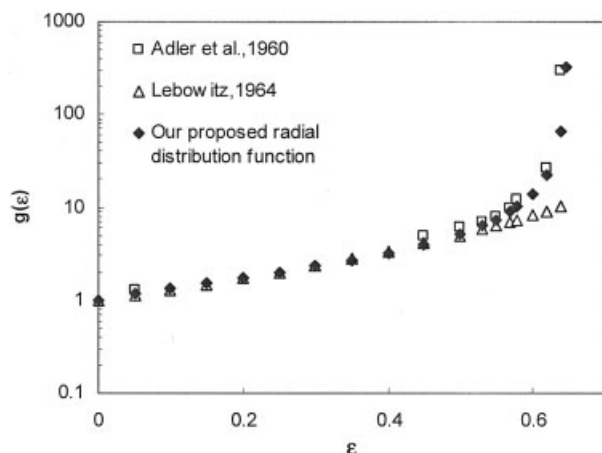


Figure 1. Comparison of the proposed radial distribution function (diamonds) for a monodisperse particulate phase with the radial distribution function of Lebowitz²⁵ (triangles) and the molecular dynamics (MD) simulation results of Alder and Wainwright²⁶ (squares).

Table 1 shows that first and second terms in the expressions of R_0 to R_{10} are not negligible; however, the third and higher-order terms are significantly lower than the first two terms. Therefore, only two terms in the cited expressions were considered.

Numerical Simulation of Simple Shear Flow

A binary solid mixture (1 and 2) with the same density and normal restitution coefficient was sheared between two infinite parallel plates set to move with relative velocities $\pm V_0/2$. The motion of the granular mixture was only in the x -direction and was considered fully developed so that all the flow parameters are a function of y . In this study x and y are the axes parallel and perpendicular to the plates, respectively, as shown in Figure 2. In this example, we are interested in the steady-state regime, where the thermal equilibrium may be reached when the viscous effect arising from continuous shearing is balanced by the dissipation resulting from collisions.

Simple shear flow is characterized by a linear profile of the velocity field (the shear rate dv/dy is constant). In this situation the external forces are neglected and the particles in the mix-

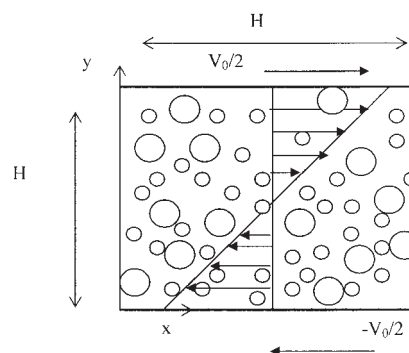


Figure 2. Simple shear flow of a binary mixture.

ture move with the same center of mass average velocity, \bar{v} . This means that the granular temperatures, solid volume fractions, and gradient of the velocities are all uniform throughout the flow zone. Therefore, energy equations for phases 1 and 2 reduce to the following nonlinear algebraic equations:

$$-\left[\mu_{11} + \frac{\alpha_{12}}{2} \left(\frac{1}{\theta_1} + \frac{1}{\theta_2}\right)\right] \left(\frac{dv}{dy}\right)^2 = N_{11} + N_{12} \quad (26)$$

$$-\left[\mu_{22} + \frac{\alpha_{12}}{2} \left(\frac{1}{\theta_1} + \frac{1}{\theta_2}\right)\right] \left(\frac{dv}{dy}\right)^2 = N_{22} + N_{21} \quad (27)$$

where

$$\mu_{11} = \left\{ \frac{5}{16d_{12}^2 g_{11}} \left[1 + \frac{4}{5} (1 + e) g_{11} \varepsilon_1 \right]^2 + \frac{4d_1(1 + e)\varepsilon_1^2 \rho g_{11}}{5m_1} \right\} \sqrt{\frac{m_1 \theta_1}{\pi}} \quad (28)$$

$$\mu_{22} = \left\{ \frac{5}{16d_{22}^2 g_{22}} \left[1 + \frac{4}{5} (1 + e) g_{22} \varepsilon_2 \right]^2 + \frac{4d_2(1 + e)\varepsilon_2^2 \rho g_{22}}{5m_2} \right\} \sqrt{\frac{m_2 \theta_2}{\pi}} \quad (29)$$

$$\alpha_{12} = \frac{\sqrt{\pi}}{48} d_{12}^4 g_{12} \frac{m_2 m_1}{m_0^2} \left(\frac{m_1 m_2}{\theta_1 \theta_2} \right)^{3/2} (1 + e) \rho^2 \varepsilon_2 \varepsilon_1 \frac{1}{5} R_1 \quad (30)$$

$$N_{ip} = \frac{3}{4} d_{ip}^2 (e + 1) g_{ip} \varepsilon_i \varepsilon_p \left(\frac{m_i m_p}{\theta_i \theta_p} \right)^{3/2} \frac{\sqrt{\pi}}{m_0} \times \left\{ B_{ip} \cdot R_5 + (e - 1) \frac{m_p}{m_0} \frac{1}{6} \cdot R_1 \right\} \quad (31)$$

N_{12} , N_{11} , and N_{22} were obtained from Eq. 31.

The granular mixture normal and shear stresses are

$$\tau_T = \sum_{i=1}^2 \sum_{p=1}^2 (\mu_{ip} + \mu_{ii}) \frac{dv}{dy} \quad (32)$$

Table 1. Comparison between Terms of the Series in the Constitutive Equations*

	Term 1	Term 1 + Term 2	Term 1 + Term 2 + Term 3
R_0	5.68e-01	6.02e-01	6.05e-01
R_1	1.89e-01	2.33e-01	2.37e-01
R_2	8.63e-02	9.96e-02	1.00e-01
R_3	1.98e-01	2.52e-01	2.52e-01
R_4	5.43e-02	7.87e-02	8.07e-02
R_5	5.18e-02	5.85e-02	5.90e-02
R_6	1.42e-02	1.68e-02	1.70e-02
R_7	8.53e-02	9.99e-02	1.00e-01
R_8	1.04e-01	1.36e-01	1.36e-01
R_9	5.18e-02	7.19e-02	7.43e-02
R_{10}	4.95e-02	6.54e-02	6.71e-02

*Data taken from Wildman and Parker¹⁷; material was balotini glass beads. $d_1 = 5$ mm, $d_2 = 4$ mm, $e = 0.91$, $\theta_1/\theta_2 = 1.41$, and $\varepsilon_1/\varepsilon_2 = 3.7$.

$$\tau_N = \sum_{i=1}^2 \sum_{p=1}^2 \left(\delta_{ip} + \frac{\varepsilon_i \rho_i}{m_i} \theta_i \right) \quad (33)$$

with

$$\mu_{ip} = \frac{\alpha_{ip}}{2} \left(\frac{1}{\theta_i} + \frac{1}{\theta_p} \right) \quad (34)$$

and

$$\delta_{ip} = \frac{d_{ip}^3 \pi}{48} g_{ip} \frac{1}{\bar{m}_0} \left(\frac{m_i m_p}{\theta_i \theta_p} \right)^{3/2} \varepsilon_i \varepsilon_p \rho_i \rho_p \left(1 + \frac{e}{m} \right) \cdot R_0 \quad (35)$$

where R_0 is defined in the Appendix.

The system of Eqs. 26 and 27 was solved numerically for θ_1 and θ_2 , for the same flow parameters used by Galvin et al.²⁴ The large particle mass m_1 is 1. The ratio of the plate spacing to the large particle diameter H/d_1 is 4.45 or 8.9, depending on the total solid volume fraction and the solid volume fraction ratio. The ratio of H/d_1 was chosen in the MD simulation to avoid cluster formation.^{24,27-29} Furthermore, the shear rate was set to a constant value of $V_0/H = \gamma = 1.0$

Results and Discussion

The calculated granular energies and the stresses for different diameter ratios using our model were compared with the Jenkins and Mancini¹⁰ theoretical results and MD simulation results of Galvin et al.²⁴ To analyze the effect of the elasticity and the concentration ratio on the granular energies, Eqs. 26 and 27 were solved simultaneously for two different volume fraction ratios $\varepsilon_1/\varepsilon_2 = 0.5$ and 1, with restitution coefficients ranging from 0.99 to 0.8, and particle diameter ratios ranging from 1 to 4. The diameter of particle 1 (large particle) was kept constant and the diameter of particle 2 (small particle) was variable.

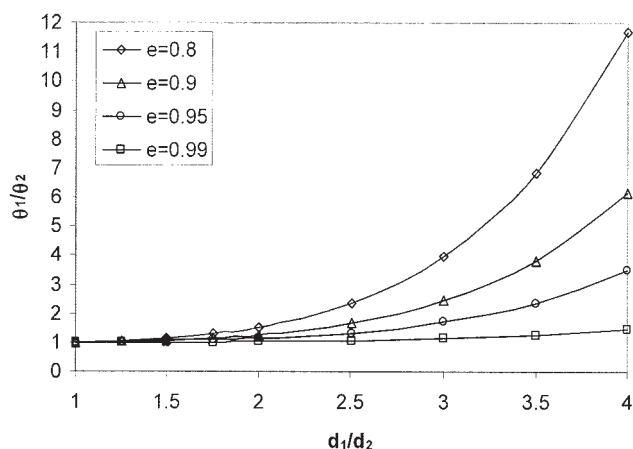


Figure 3. Variation of the granular energy ratio with the diameter ratio for different restitution coefficients.

$\rho_1/\rho_2 = 1$, $\varepsilon_T = 0.5$, and $\varepsilon_1/\varepsilon_2 = 0.5$. The subscripts 1 and 2 denote large and small particles, respectively.

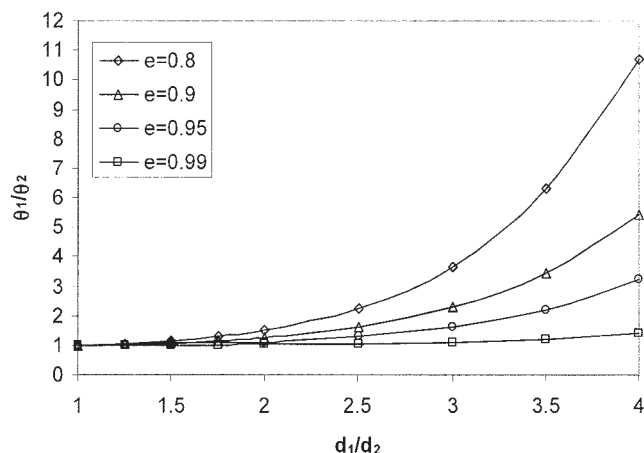


Figure 4. Variation of the granular energy ratio with the diameter ratio for different restitution coefficients.

$\rho_1/\rho_2 = 1$, $\varepsilon_T = 0.5$, and $\varepsilon_1/\varepsilon_2 = 1$.

Figure 3 shows the variation of the fluctuating energy ratio with the particle size ratio at different restitution coefficients for $\varepsilon_1/\varepsilon_2 = 0.5$. Our model predicts well the non-equipartition of energy of the two interacting particles for inelastic collisions. As observed by several investigations in the literature,^{29,30} the fluctuating granular energy of the large particles increases relative to that of the small particles with an increase in large to small diameter ratio.

In the range of parameters investigated, equipartition was observed in two cases; first, when the restitution coefficient is >0.99 and, second, when the two particles have the same mechanical properties ($\rho_1 = \rho_2$ and $d_1 = d_2$). We noticed that the restitution coefficient is the most important parameter responsible for non-equipartition. The effect of restitution coefficient on the deviation of granular temperature of two particles from each other is enhanced by the size disparity. For example, for $e = 0.99$, the ratio θ_1/θ_2 increases very slowly with the size ratio; however, for $e = 0.8$, a strong increase was observed for higher particle diameter ratios. Our results also showed the condition upon which the equipartition of energy assumption could be reasonable, which is for a diameter ratio < 2 and restitution coefficient of >0.95 . Our calculation also showed that smaller particles dissipate more energy when interacting with larger particles through inelastic collisions. This behavior is more pronounced when the size ratio increases and the restitution coefficient decreases.

Figure 4 exhibits the variation of the fluctuating energy ratio with the particle size ratio at different restitution coefficients for $\varepsilon_1/\varepsilon_2 = 1$. Similar to Figure 3, the fluctuating energy ratio increases with the diameter ratio and decreases with the restitution coefficient. In the range of the parameters studied, Figures 3 and 4 show that the fluctuating energy ratio is weakly

Table 2. Dependency of the Granular Temperature Ratio on the Composition, for a Restitution Coefficient of 0.8, $d_1/d_2 = 2$, $\rho_1/\rho_2 = 1$, and $\varepsilon_T = 0.5$

$\varepsilon_1/\varepsilon_2$	0.5	1	2
θ_1/θ_2	1.510	1.482	1.450

Table 3. Dependency of the Granular Temperature Ratio on the Size Ratio, for a Restitution Coefficient of 0.8, $\varepsilon_1/\varepsilon_2 = 1$, $m_1/m_2 = 1$, and $\varepsilon_T = 0.3$

d_1/d_2	1	2	4
θ_1/θ_2	1.000	1.061	1.081

dependent on the concentration ratio of two particulate phases. For example, at $e = 0.8$ and diameter ratio of 2, the granular energy ratio changes very sensitively with the composition ($\varepsilon_1/\varepsilon_2$) (see Table 2). This observation is also consistent with the experiment of Feitosa and Menon¹⁸ that showed that the granular temperature ratio is insensitive to the composition.

Our model was also applied to a mixture of equal mass and two different size particles (size ratio varying from 1 to 4), for $e = 0.8$, which showed that the granular energy ratio θ_1/θ_2 of the two phases varied by about 8% between $d_1/d_2 = 1$ and $d_1/d_2 = 4$, as shown in Table 3. This result is in good qualitative agreement with the experimental results of Feitosa and Menon¹⁸ that showed that energy non-equipartition prevailed when the mass ratio is significantly greater than one; this behavior is the same as that in our model prediction.

Figures 5 and 6 show the comparison between our calculated fluctuating energy ratio as a function of the diameter ratio with the MD simulation and the theoretical results of Jenkins and Mancini,¹⁰ at $\varepsilon_T = 0.3$, $\varepsilon_1/\varepsilon_2 = 0.5$, and two restitution coefficients of 0.8 and 0.95, respectively. The results given by our model compared very well with the MD simulation results than with those of Jenkins and Mancini.¹⁰ The deviation of the Jenkins and Mancini theory from the MD simulation and our results is more pronounced for low restitution coefficients and high diameter ratios. At a diameter ratio < 1.5 , both theories exhibit good agreement with the MD simulation results, but beyond this ratio, more deviation was observed.

Figures 7 and 8 are similar to Figures 5 and 6, but for $\varepsilon_T = 0.5$ and $\varepsilon_1/\varepsilon_2 = 0.5$. Again, the results given by our model compared better with the MD simulation results of Galvin et

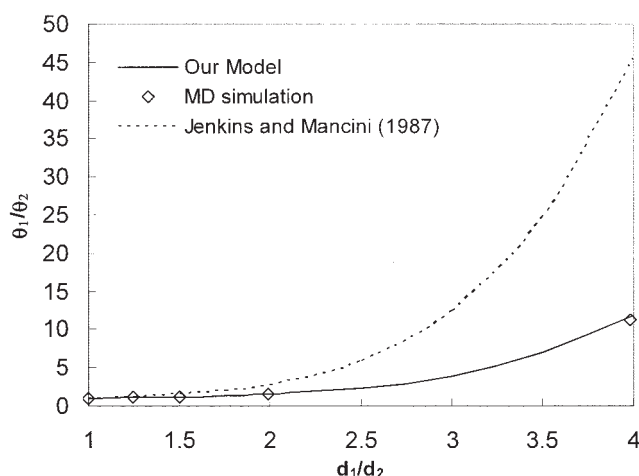


Figure 5. Variation of the granular energy ratio with the diameter ratio for $e = 0.8$, $\rho_1/\rho_2 = 1$, $\varepsilon_T = 0.3$, and $\varepsilon_1/\varepsilon_2 = 0.5$.

Comparison of our theory (solid line) with the theory of Jenkins and Mancini¹⁰ (dashed line) and the MD simulation results of Galvin et al.²⁴ (diamonds).

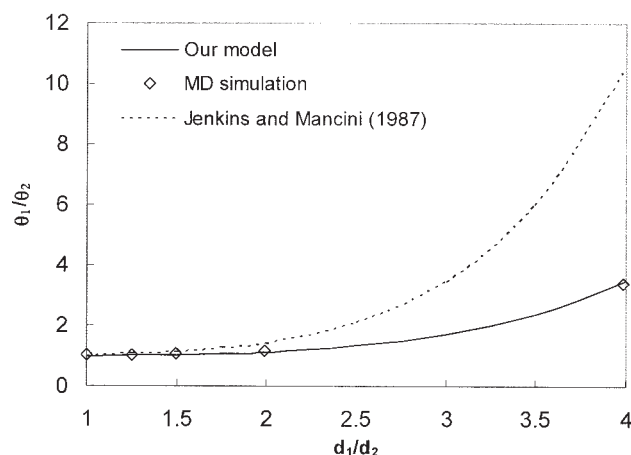


Figure 6. Variation of the granular energy ratio with the diameter ratio for $e = 0.95$, $\rho_1/\rho_2 = 1$, $\varepsilon_T = 0.3$, and $\varepsilon_1/\varepsilon_2 = 0.5$.

Comparison of our theory (solid line) with the theory of Jenkins and Mancini¹⁰ (dashed line) and the MD simulation results of Galvin et al.²⁴ (diamonds).

al.²⁴ than with those of Jenkins and Mancini.¹⁰ However, we notice that at this total solid volume fraction ($\varepsilon_T = 0.5$), our model underpredicts the energy non-equipartition obtained by the MD simulation.

The deviation of the Jenkins and Mancini theory from the MD simulation results is expected because they assumed that the deviation of the fluctuating energy of each particle from the mean is infinitesimal. In the context of the kinetic theory, the only existing models that account for non-equipartition in the limit of the Maxwellian velocity distribution were developed by Jenkins and Mancini¹⁰ and Huilin et al.^{19,20} Comparison of our model with the Jenkins and Mancini model showed that our calculated values were in better agreement with the results of the MD simulation. Comparison with the Huilin et al.^{19,20} model could not be made because, in their model, the information on how the kinetic energy is distributed between the two colliding particles cannot be calculated. Furthermore, in

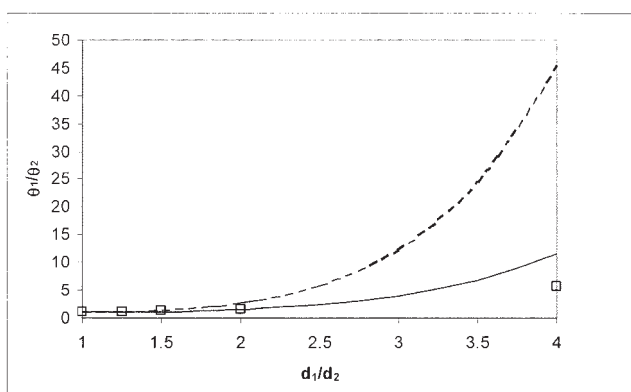


Figure 7. Variation of the granular energy ratio with the diameter ratio for $e = 0.8$, $\varepsilon_T = 0.5$, and $\varepsilon_1/\varepsilon_2 = 0.5$.

Comparison of our theory (solid line) with the theory of Jenkins and Mancini¹⁰ (dashed line) and the MD simulation results of Galvin et al.²⁴ (squares).

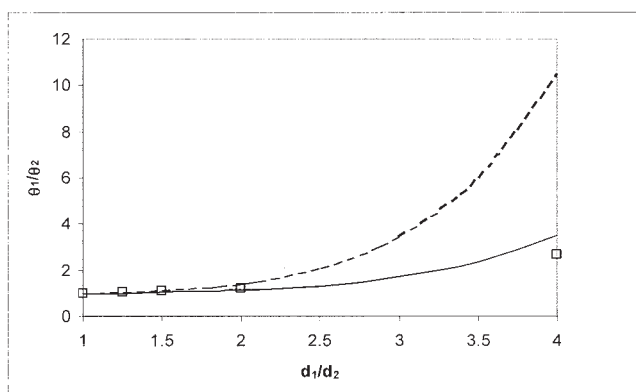


Figure 8. Variation of the granular energy ratio with the diameter ratio for $e = 0.95$, $\varepsilon_T = 0.5$, and $\varepsilon_1/\varepsilon_2 = 0.5$.

Comparison of our theory (solid line) with the theory of Jenkins and Mancini¹⁰ (dashed line) and the MD simulation results of Galvin et al.²⁴ (squares).

the case of simple shear flow, we noticed that the expression of energy dissipation using the Huilin et al.^{19,20} study results in the same values for the two colliding particles regardless of their properties.

Figure 9 shows that the mixture granular energy $[\theta_m = (n_1\theta_1 + n_2\theta_2)/(n_1 + n_2)]$ decreases with increasing the diameter ratio for $\varepsilon_T = 0.3$, $\varepsilon_1/\varepsilon_2 = 0.5$, and $e = 0.95$. This behavior was expected, at constant composition: increasing the diameter ratio is equivalent to increasing the number of smaller particles in the system, thus lowering their fluctuations. This is explained by the increase in the frequency of the collisions with the increase in the number of particles in the system and, thus, damping the fluctuations of the particulate phase as a whole. Comparison between the present theory and the simulation shows a good quantitative agreement.

Figure 10 shows the variation of the dimensionless normal and shear stresses with the diameter ratio, for a mixture of particles of equal density and composition. Our results clearly showed that the normal and shear stresses decrease with an increase in the particle size ratio in a binary mixture; in other

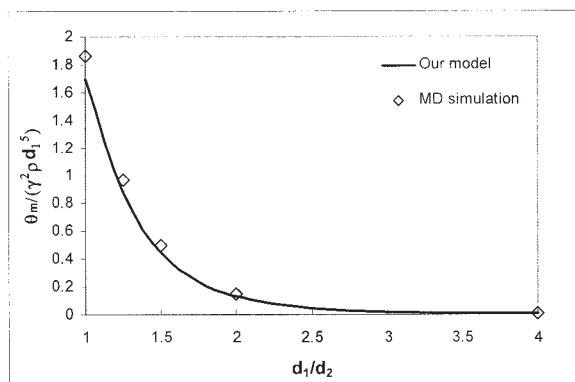


Figure 9. Variation of the granular energy ratio with the diameter ratio for $e = 0.95$, $\rho_1/\rho_2 = 1$, $\varepsilon_T = 0.3$, and $\varepsilon_1/\varepsilon_2 = 0.5$.

Comparison of our theory (solid line) with the MD simulation results of Galvin et al.²⁴ (diamonds).

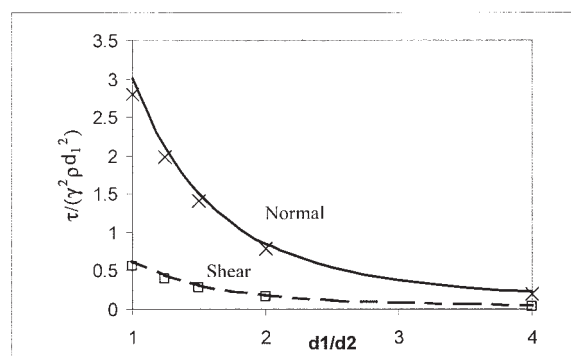


Figure 10. Variation of the dimensionless stresses with the diameter ratio for $e = 0.95$, $\varepsilon_T = 0.3$, and $\varepsilon_1/\varepsilon_2 = 0.5$.

Comparison of our theory (lines) with the MD simulation results of Galvin et al.²⁴ (symbols).

words, our model predicts the maximum normal and shear stresses for monosize larger particles. This behavior was also confirmed by the experiment of Savage and Sayed⁹ that indicated that the stresses in a binary mixture (same density, different sizes) were about five times lower than those for a monosize mixture. We also compared the normal and shear stresses with the MD simulation results of Galvin et al.²⁴ when Maxwellian and non-Maxwellian velocity distributions were assumed. Our model shows a good agreement with the MD simulation for non-Maxwellian velocity distribution. However, the normal and shear stresses were underpredicted when assuming Maxwellian velocity distribution.

Figure 11 depicts the variation of the dimensionless normal and shear stresses with density ratio varying between 0.1 and 0.75, in the case of $d_1/d_2 = 1.5$, $\varepsilon_T = 0.3$, $\varepsilon_1/\varepsilon_2 = 1$, and $e = 0.95$. The granular flow shows less resistance to the shearing motion when the density of larger particle increases.

Conclusion

A model based on the kinetic theory of mixture of hard and smooth spherical particles was developed to predict the behav-

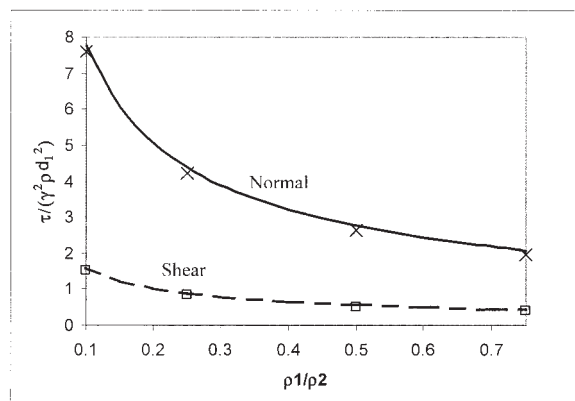


Figure 11. Variation of the dimensionless stresses with the particle density ratio for $e = 0.95$, $\varepsilon_T = 0.3$, $\varepsilon_1/\varepsilon_2 = 1$, and $d_1/d_2 = 1.5$.

Comparison of our theory (lines) with the MD simulation results of Galvin et al.²⁴ (symbols).

ior of multitype particle flow systems. In the range of parameters studied this model showed that the assumption of uniform equilibrium at the interface is reasonable and results in significant reduction in complexity of the mathematical derivation of the model.

Our proposed radial distribution function at contact, based on the modification of Lebowitz²⁵ for a mixture of hard and smooth spherical particles, predicts values at a broad range of solid volume fractions.

Our model was applied to a simple shear flow of a binary mixture. Our calculated values showed that for $\rho_1/\rho_2 = 1$ the variation of the granular energy ratio of two particulate phases depends on both the diameter ratio and the inelasticity of the particles. This observation is similar to the computer simulation results in the literature.

In the range of parameters investigated, our calculated fluctuating energy ratio and the stresses of the particulate phases as a function of the diameter ratio and density ratio agreed well with the molecular dynamic simulation of Galvin et al.²⁴ Our calculated values also compared qualitatively well with the experimental data of Savage and Sayed,⁹ Feitosa and Menon,¹⁸ and simulations of Alam and Luding.³⁰ In general our model for multitype particles with non-Maxwellian velocity distribution function and energy non-equipartition assumptions showed that it is capable of describing not only granular simple shear but also, in principle, more complex reacting flow systems.

Acknowledgments

The authors thank Dr. C. M. Hrenya for providing them data in useful form to compare them with their results, and the Energy and Power Center at IIT for providing financial support.

Notation

(In the following, the subscript s can be either i or p .)

\vec{c}_s	= instantaneous particle velocity
\vec{C}_s	= peculiar particle velocity
d_s	= diameter of the particle
$d_{ip} = (d_i + d_p)/2$	= average diameter of particles i and p
e_{ip}	= restitution coefficient
\vec{F}_{Dip}	= momentum source (drag between solid phases)
f_s^0	= Maxwellian velocity distribution function
f_s^1	= single velocity distribution function
f_{ip}^2	= pair velocity distribution function
g_{ip}	= radial distribution function at contact between particles i and p
g_{ss}	= radial distribution function at contact between particles of the same phase
H	= gap between the two plates
\vec{I}	= identity tensor
$\vec{k} = \vec{k}_{ip}$	= unit vector connecting the centers of the two particles
m_s	= mass of the particle of phase s
$m_0 = m_i + m_p$	= total mass of two colliding particles
n_s	= number density of phase s
N_{ip}	= energy dissipation
\vec{P}_c	= collisional pressure tensor
\vec{P}_k	= kinetic pressure tensor
\vec{q}_c	= collisional flux
\vec{q}_k	= kinetic flux
\vec{v}	= center of mass mean velocity
\vec{v}_s	= mean velocity of phase s
\vec{V}_0	= velocity of the plates

Greek letters

χ_{ip}	= collisional flux
ε_s	= solid volume fraction of phase s
ε_T	= total solid volume fraction
ϕ_s	= perturbation to Maxwellian distribution function
γ	= shear rate
γ_{ip}	= collisional source
μ_{ss}	= granular viscosity of phase s
μ_{ip}	= mixture granular viscosity
ρ_s	= solid density of phase s
θ_s	= fluctuating granular energy
θ_m	= mixture fluctuating granular energy
τ_N	= mixture normal stress
τ_t	= mixture shear stress
ψ_s	= property of particle

Subscripts

1	= large
2	= small
T	= total
s	= phase s (may be i or p)

Literature Cited

- Chapman S, Cowling TG. *The Mathematical Theory of Non-Uniform Gases*. Cambridge, UK: Cambridge Univ. Press; 1970.
- Savage SB, Jeffrey DJ. The stress tensor in a granular flow at high shear rates. *J Fluid Mech.* 1981;110:255-272.
- Jenkins JT, Savage SB. A theory for the rapid flow of identical, smooth, nearly elastic, spherical particles. *J Fluid Mech.* 1983;130:187-201.
- Lun CKK, Savage SBD, Jeffrey J, Chepurniy N. Kinetic theories for granular flow: Inelastic particles in couette flow and slightly inelastic particles in a general flowfield. *J Fluid Mech.* 1984;140:223-256.
- Jenkins JT, Richman MW. Boundary conditions for plane flows of smooth, nearly elastic, circular disks. *J Fluid Mech.* 1986;171:53-68.
- Jenkins JT, Richman MW. Kinetic theory for plane flows of a dense gas of identical, rough, inelastic, circular disks. *Phys Fluids.* 1985;28:3485-3494.
- Hopkins MA, Shen HH. A Monte Carlo solution for rapidly shearing granular flows based on the kinetic theory of dense gases. *J Fluid Mech.* 1992;244:477-491.
- Arastoopour H, Lin SC, Weil SA. Analysis of vertical pneumatic conveying of solids using multiphase flow models. *AIChE J.* 1982;28:467-473.
- Savage SB, Sayed M. Stresses developed by dry cohesionless granular materials sheared in annular shear cell. *J Fluid Mech.* 1984;142:391-430.
- Jenkins JT, Mancini F. Balance laws and constitutive relations for plane flows of a dense binary mixture of smooth, nearly elastic, circular disks. *J Appl Mech.* 1987;54:27-34.
- Jenkins JT, Mancini F. Kinetic theory for binary mixtures of smooth, nearly elastic spheres. *Phys Fluids A.* 1989;1:2050-2057.
- Arnason BO, Willits JT. Thermal diffusion in binary mixtures of smooth, nearly elastic spheres with and without gravity. *Phys Fluids.* 1998;10:1324-1328.
- Willits JT, Arnason BO. Kinetic theory of a binary mixture of nearly elastic disks. *Phys Fluids.* 1999;11:3116-3122.
- Alam M, Willits JT, Arnason BO, Luding S. Kinetic theory of a binary mixture of nearly elastic disks with size and mass disparity. *Phys Fluids.* 2002;14:4085-4087.
- Zamankhan P. Kinetic theory of multicomponents dense mixtures of slightly inelastic spherical particles. *Phys Rev E.* 1995;52:5706-5713.
- Garzó V, Dufty J. Homogeneous cooling state for a granular mixture. *Phys Rev E.* 1999;60:5706-5713.
- Wildman RD, Parker DJ. Coexistence of two granular temperatures in binary vibrofluidized beds. *Phys Rev Lett.* 2002;88:(064301)1-(064301)4.

18. Feitosa K, Menon N. Breakdown of energy equipartition in 2d binary vibrated granular gas. *Phys Rev Lett*. 2002;88:(031301)1-(031301)4.
19. Huilin L, Gidaspow D, Manger E. Kinetic theory of fluidized binary granular mixtures. *Phys Rev E*. 2001;64:(061301)1-(061301)8.
20. Huilin L, Wenti L, Rushan B, Lidan Y, Gidaspow D. Kinetic theory of fluidized binary granular mixtures with unequal granular temperature. *Physica A*. 2000;284:265-276.
21. Manger E. *Modeling and Simulation of Gas/Solids Flow in Curvilinear Coordinates*. PhD Thesis. Trondheim, Norway: Institutt for Prosesssteknologi (ITP)/NTNU; 1996.
22. Garzó V, Dufty J. Hydrodynamics for granular binary mixture at low density. *Phys Fluids*. 2002;14:1476-1490.
23. Ferziger JH, Kaper HG. *Mathematical Theory of Transport Processes in Gases*. Amsterdam: North-Holland; 1972.
24. Galvin JE, Dahl SR, Hrenya CM. On the role of non-equipartition in the dynamics of rapidly flowing granular mixtures. *J Fluid Mech*. 2005;258:207-232.
25. Lebowitz JL. Exact solution of generalized Percus–Yevick equation for a mixture of hard spheres. *Phys Rev*. 1964;133:895-899.
26. Alder BJ, Wainwright TE. Studies in molecular dynamics. II. Behavior of small number of elastic spheres. *J Chem Phys*. 1960;33:2363-2382.
27. Hopkins MA, Louge MY. Inelastic microstructure in rapid granular flows of smooth disks. *Phys Fluids*. 1991;A3:47-57.
28. Liss ED, Glasser BJ. The influence of clusters on the stress in sheared granular material. *Powder Technol*. 2001;116:116-132.
29. Clelland R, Hrenya CM. Simulation of a binary-sized mixture of inelastic grains in rapid shear flow. *Phys Rev E*. 2002;65:(031301)1-(031301)9.
30. Alam M, Luding S. Rheology of bidisperse granular mixtures via event driven simulations. *J Fluid Mech*. 2002;476:69-103.

Appendix

Expanding the functions in Eq. 20 in Taylor series about \tilde{r} , and neglecting all terms involving derivative of order higher than the first and product of derivative, Eq. 20 can be rewritten as

$$-\sum_{p=1}^N n_p n_p I(\phi_{ip}) = (Df_i)^0 - \sum_{p=1}^N J(f_i^0, f_p^0) \quad (A1)$$

where I is the integral operator^{1,23}:

$$\begin{aligned} f_{ip}^{02} = g_{ip} n_p \left(\frac{m_i m_p}{4\pi\theta_p} \right)^{3/2} \times \exp \left[- \left(\frac{m_i}{2\theta_i} \left(\tilde{V}_{ip} + \frac{m_p}{m_0} \tilde{C}_{ip} \right)^2 + \frac{m_p}{2\theta_p} \left(\tilde{V}_{ip} - \frac{m_i}{m_0} \tilde{C}_{ip} \right)^2 \right) \right] & \left\{ 1 + \frac{d_{ip} \tilde{k}}{2} \left[\nabla \ln \frac{n_p}{n_i} + \frac{1}{2} \left(\frac{m_p}{\theta_p^2} \left(\tilde{V}_{ip} - \frac{m_i}{m_0} \tilde{C}_{ip} \right)^2 - \frac{3}{\theta_p} \right) \right. \right. \\ & \times \nabla \theta_p - \frac{1}{2} \left(\frac{m_i}{\theta_i^2} \left(\tilde{V}_{ip} + \frac{m_p}{m_0} \tilde{C}_{ip} \right)^2 - \frac{3}{\theta_i} \right) \nabla \theta_i + \left. \left(\frac{m_p}{\theta_p} \nabla \cdot \tilde{v}_p \left(\tilde{V}_{ip} - \frac{m_i}{m_0} \tilde{C}_{ip} \right) - \frac{m_i}{\theta_i} \nabla \cdot \tilde{v}_i \left(\tilde{V}_{ip} + \frac{m_p}{m_0} \tilde{C}_{ip} \right) \right) \right] \right\} \quad (A7) \end{aligned}$$

where $\tilde{G} = \tilde{C}_i + (m_p/m_0)\tilde{C}_{ip}$ is the center of mass velocity, $\tilde{v}_{ip} = \tilde{v}_i - \tilde{v}_p$ is the relative mean velocity, and $m_0 = m_i + m_p$ is the total mass of the two colliding particles.

The expanded expression A6 was used to calculate collisional fluxes $[\chi_{cip}(m_i \tilde{C}_i), \chi_{cip}(m_i \tilde{C}_i^2)]$ and sources $[\gamma_{cip}(m_i \tilde{C}_i), \gamma_{cip}(m_i \tilde{C}_i^2)]$. In this calculation, we assumed that the average particle velocity was unaffected by collision and that the square of the relative average velocity was negligible.

$$I(\phi_{ip}) = \frac{1}{n_i n_p} \iiint g_{ip} (\phi_i + \phi_p - \phi'_i - \phi'_p) \times f_{ip}^0 f_{ip}^0 (\tilde{C}_{ip} \cdot \tilde{k}) d\tilde{k} d\tilde{C}_i d\tilde{C}_p \quad (A2)$$

$$(Df_i)^0 = f_i^0 \left(\frac{\partial}{\partial t} + \tilde{C}_i \nabla_r + \frac{\tilde{F}_{ext}}{m_i} \nabla_c \right) \ln f_i^0 \quad (A3)$$

and

$$J(f_{ip}^0, f_p^0) = d_{ip}^3 \iiint g_{ip} f_{ip}^0 f_p^0 \tilde{k} \cdot \nabla \ln(f_{ip}^0 f_p^0 g_{ip}) (\tilde{C}_{ip} \cdot \tilde{k}) d\tilde{k} d\tilde{C}_i \quad (A4)$$

To solve the first-order approximation (Eq. 20), we must first solve the zeroth-order approximation.

(1) Zeroth-order approximation to f_i^1

At this order the single velocity distribution function is Maxwellian

$$\begin{aligned} f_{ip}^{02} \left(\tilde{C}_i, \tilde{r} - \frac{d_{ip}}{2} \tilde{k}; \tilde{C}_p, \tilde{r} + \frac{d_{ip}}{2} \right) \\ = g_{ip}(\epsilon_i, \epsilon_p) \cdot f_i^0 \left(\tilde{C}_i, \tilde{r} - \frac{d_{ip}}{2} \tilde{k} \right) \cdot f_p^0 \left(\tilde{C}_p, \tilde{r} + \frac{d_{ip}}{2} \right) \quad (A5) \end{aligned}$$

To determine the constitutive relations, the complete pair distribution function (Eq. A5) was expanded in a Taylor series about $\tilde{r} + (d_{ip}/2)\tilde{k}$ for $f_i^0[\tilde{C}_i, \tilde{r} - (d_{ip}/2)\tilde{k}]$ and $\tilde{r} - (d_{ip}/2)\tilde{k}$ for $f_p^0[\tilde{C}_p, \tilde{r} + (d_{ip}/2)\tilde{k}]$. Considering only the first-order terms, f_{ip}^0 may be expressed as

$$\begin{aligned} f_{ip}^{02} = f_{ip}^{02} \left(\tilde{C}_i, \tilde{r} - \frac{d_{ip}}{2} \tilde{k}; \tilde{C}_p, \tilde{r} + \frac{d_{ip}}{2} \right) \\ = g_{ip} \left(f_{ip}^0 + \frac{1}{2} d_{ip} \tilde{k} f_{ip}^0 \cdot \nabla \ln \frac{f_p^0}{f_i^0} \right) \quad (A6) \end{aligned}$$

where $f_i^0 = f_i^0(\tilde{C}_i, \tilde{r})$ and $f_p^0 = f_p^0(\tilde{C}_p, \tilde{r})$.

Equation A6 was rewritten in terms of the relative velocities $\tilde{C}_{ip} = \tilde{C}_i - \tilde{C}_p$ and $\tilde{V}_{ip} = \tilde{G} - \tilde{v}_i + (m_p/m_0)\tilde{v}_{ip}$ as follows:

Because there is no closed form for the integrals involved in this derivation, integrals were expanded in the Taylor series as done by Manger.²¹ The collisional pressure tensor, particulate phase momentum interaction, energy dissipation, and collisional heat flux were carried out and expressed as follows:

Zeroth-Order Particulate Phase Collisional and Kinetic Pressure Tensor

$$\bar{P}_{cip}^0 = \frac{d_{ip}^3}{48} g_{ip} \frac{m_i m_p}{m_0} \left(\frac{m_i m_p}{\theta_i \theta_p} \right)^{3/2} n_i n_p (1 + e_{ip})$$

$$\times \left\{ \pi R_0 \bar{I} - \sqrt{\pi} d_{ip} \frac{m_i m_p}{m_0} \frac{1}{3} \left[\frac{6}{5} \left(\frac{\nabla \cdot \tilde{v}_p}{\theta_p} + \frac{\nabla \cdot \tilde{v}_i}{\theta_i} \right) + \left(\frac{\nabla \cdot \tilde{v}_p}{\theta_p} + \frac{\nabla \cdot \tilde{v}_i}{\theta_i} \right) \bar{I} \right] R_1 \right\} \quad (A8)$$

$$\bar{P}_{ki}^0 = \frac{\rho_i \varepsilon_i}{m_i} \langle \tilde{C}_i \tilde{C}_i \rangle^0 = \frac{\rho_i \varepsilon_i}{m_i} \theta_i \quad (A9)$$

Energy Dissipation

$$N_{ip} = \frac{3}{4} d_{ip}^2 (e_{ip} + 1) g_{ip} n_i n_p \left(\frac{m_i m_p}{\theta_i \theta_p} \right)^{3/2} \frac{m_i m_p}{m_0} \left\{ B_{ip} \sqrt{\pi} \cdot R_5 + \frac{3 d_{ip} \pi}{40} \left(\frac{m_p \nabla \cdot \tilde{v}_p}{\theta_p} - \frac{m_i \nabla \cdot \tilde{v}_i}{\theta_i} \right) \cdot R_{10} \right.$$

$$+ B_{ip} \frac{d_{ip} \pi}{4} \frac{m_i m_p}{m_0} \left(\frac{\nabla \cdot \tilde{v}_p}{\theta_p} + \frac{\nabla \cdot \tilde{v}_i}{\theta_i} \right) \cdot R_4 + (e_{ip} - 1) \frac{m_p}{m_0} \left[\frac{\sqrt{\pi}}{6} \cdot R_1 + B_{ip} \frac{d_{ip} \pi}{16} \left(\frac{m_p \nabla \cdot \tilde{v}_p}{\theta_p} - \frac{m_i \nabla \cdot \tilde{v}_i}{\theta_i} \right) \cdot R_4 - \frac{d_{ip} \pi}{48} \frac{m_i m_p}{m_0} \left(\frac{\nabla \cdot \tilde{v}_p}{\theta_p} + \frac{\nabla \cdot \tilde{v}_i}{\theta_i} \right) \cdot R_3 \right] \left. \right\} \quad (A11)$$

Zeroth-Order Collisional Heat Flux

$$\tilde{q}_{cip}^0 = d_{ip}^3 \frac{m_p m_i}{2 m_0} (1 + e_{ip}) \left(\frac{m_i m_p}{\theta_i \theta_p} \right)^{3/2} n_i n_p g_{ip} \times \left\{ \frac{d_{ip} \sqrt{\pi}}{16} \left[B_{ip} \left(\nabla \ln \frac{n_p}{n_i} + \frac{3}{2} \nabla \ln \frac{\theta_i}{\theta_p} \right) R_5 + \frac{B_{ip}}{8} \left(\frac{m_p \nabla \theta_p}{\theta_p^2} - \frac{m_i \nabla \theta_i}{\theta_i^2} \right) R_6 \right. \right.$$

$$+ B_{ip} \frac{m_p m_i}{m_0^2} \left(\frac{m_i \nabla \theta_p}{\theta_p^2} - \frac{m_p \nabla \theta_i}{\theta_i^2} \right) R_7 + \frac{m_p m_i}{2 m_0} \left(\frac{\nabla \theta_p}{\theta_p^2} - \frac{\nabla \theta_i}{\theta_i^2} \right) R_9 \left. \right] + \frac{m_p}{8 m_0} (1 - e_{ip}) \left[\frac{d_{ip} \pi}{6} \left(\nabla \ln \frac{n_p}{n_i} + \frac{3}{2} \nabla \ln \frac{\theta_i}{\theta_p} \right) R_1 \right.$$

$$+ \frac{3 \pi}{10} (\tilde{v}_i - \tilde{v}_p) R_0 + \frac{d_{ip} \sqrt{\pi}}{8} \left(\frac{m_p \nabla \theta_p}{\theta_p^2} - \frac{m_i \nabla \theta_i}{\theta_i^2} \right) R_9 + \frac{d_{ip} \sqrt{\pi} m_i^2}{2 m_0^2} \left(\frac{m_i \nabla \theta_p}{\theta_p^2} - \frac{m_p \nabla \theta_i}{\theta_i^2} \right) R_8 + d_{ip} \sqrt{\pi} B_{ip} \frac{m_p m_i}{m_0} \left(\frac{\nabla \theta_p}{\theta_p^2} + \frac{\nabla \theta_i}{\theta_i^2} \right) R_7 \left. \right] \quad (A12)$$

where e_{ip} is the normal restitution coefficient between particles i and p :

$$A_{ip} = \frac{m_i \theta_p + m_p \theta_i}{2 \theta_i \theta_p} \quad B_{ip} = \frac{m_i m_p (\theta_p - \theta_i)}{2 m_0 \theta_i \theta_p}$$

$$D_{ip} = \frac{m_i m_p (m_p \theta_p + m_i \theta_i)}{2 m_0^2 \theta_i \theta_p} \quad (A13)$$

$$R_0 = \frac{1}{A_{ip}^{3/2} D_{ip}^{5/2}} + \frac{15 B_{ip}^2}{2 A_{ip}^{5/2} D_{ip}^{7/2}} + \frac{175 B_{ip}^4}{8 A_{ip}^{7/2} D_{ip}^{9/2}} + \dots \quad (A14)$$

$$R_1 = \frac{1}{A_{ip}^{3/2} D_{ip}^3} + \frac{9 B_{ip}^2}{A_{ip}^{5/2} D_{ip}^4} + \frac{30 B_{ip}^4}{2 A_{ip}^{7/2} D_{ip}^5} + \dots \quad (A15)$$

Momentum Interaction

$$\tilde{F}_{Dip} = \frac{d_{ip}^2}{4} \frac{m_i m_p}{m_0} g_{ip} (1 + e_{ip}) n_i n_p \left(\frac{m_i m_p}{\theta_i \theta_p} \right)^{3/2}$$

$$\times \left\{ \sqrt{\pi} R_2 \cdot (\tilde{v}_p - \tilde{v}_i) + \frac{d_{ip} \pi}{12} R_0 \left(\nabla \ln \frac{n_i}{n_p} - \frac{3}{2} \nabla \ln \frac{\theta_i}{\theta_p} \right) + \frac{d_{ip} \pi}{16} \left[\left(\frac{m_p \nabla \theta_p}{\theta_p^2} - \frac{m_i \nabla \theta_i}{\theta_i^2} \right) R_{10} + \frac{5 m_i m_p}{192 m_0^2} \left(\frac{m_i \nabla \theta_p}{\theta_p^2} - \frac{m_p \nabla \theta_i}{\theta_i^2} \right) R_3 \right. \right.$$

$$\left. \left. + \frac{5 m_i m_p}{96 m_0} B_{ip} \left(\frac{\nabla \theta_p}{\theta_p^2} + \frac{\nabla \theta_i}{\theta_i^2} \right) R_4 \right] \right\} \quad (A10)$$

$$R_2 = \frac{1}{2 A_{ip}^{3/2} D_{ip}^2} + \frac{3 B_{ip}^2}{A_{ip}^{5/2} D_{ip}^3} + \frac{15 B_{ip}^4}{2 A_{ip}^{7/2} D_{ip}^4} + \dots \quad (A16)$$

$$R_3 = \frac{1}{A_{ip}^{3/2} D_{ip}^{7/2}} + \frac{21 B_{ip}^2}{2 A_{ip}^{5/2} D_{ip}^{9/2}} + \frac{315 B_{ip}^4}{8 A_{ip}^{7/2} D_{ip}^{11/2}} + \dots \quad (A17)$$

$$R_4 = \frac{3}{A_{ip}^{5/2} D_{ip}^{7/2}} + \frac{35 B_{ip}^2}{2 A_{ip}^{7/2} D_{ip}^{9/2}} + \frac{441 B_{ip}^4}{8 A_{ip}^{9/2} D_{ip}^{11/2}} + \dots \quad (A18)$$

$$R_5 = \frac{1}{A_{ip}^{5/2} D_{ip}^3} + \frac{5 B_{ip}^2}{A_{ip}^{7/2} D_{ip}^4} + \frac{14 B_{ip}^4}{A_{ip}^{9/2} D_{ip}^5} + \dots \quad (A19)$$

$$R_6 = \frac{1}{A_{ip}^{7/2} D_{ip}^3} + \frac{7 B_{ip}^2}{A_{ip}^{9/2} D_{ip}^4} + \frac{126 B_{ip}^4}{5 A_{ip}^{11/2} D_{ip}^5} + \dots \quad (A20)$$

$$R_7 = \frac{3}{2A_{ip}^{5/2}D_{ip}^4} + \frac{10B_{ip}^2}{A_{ip}^{7/2}D_{ip}^5} + \frac{35B_{ip}^4}{A_{ip}^{9/2}D_{ip}^6} + \dots \quad (A21)$$

$$R_8 = \frac{1}{2A_{ip}^{3/2}D_{ip}^4} + \frac{6B_{ip}^2}{A_{ip}^{5/2}D_{ip}^5} + \frac{25B_{ip}^4}{A_{ip}^{7/2}D_{ip}^6} + \dots \quad (A22)$$

$$R_9 = \frac{1}{A_{ip}^{5/2}D_{ip}^3} + \frac{15B_{ip}^2}{A_{ip}^{7/2}D_{ip}^4} + \frac{70B_{ip}^4}{A_{ip}^{9/2}D_{ip}^5} + \dots \quad (A23)$$

$$R_{10} = \frac{1}{A_{ip}^{5/2}D_{ip}^{5/2}} + \frac{25B_{ip}^2}{2A_{ip}^{7/2}D_{ip}^{7/2}} + \frac{1225B_{ip}^4}{24A_{ip}^{9/2}D_{ip}^{9/2}} + \dots \quad (A24)$$

$$\nabla^s \vec{v} = \frac{1}{2} [\nabla \vec{v} + (\nabla \vec{v})^T] - \frac{1}{3} (\nabla \vec{v} : \bar{I}) \bar{I} \quad (A25)$$

where the superscript T indicates the transpose and \bar{I} is the identity tensor.

First-order approximation to f_i^1

In this work, we are trying to give a general theory that accounts for both energy non-equipartition and non-Maxwellian velocity distribution. As mentioned in the introduction, the interaction between the phases is at the interface. To develop a system of equations that is manageable to derive, we assumed the deviation from Maxwellian velocity distribution is in each phase and at the interface the velocity distribution function is Maxwellian or zeroth order.

For each individual phase i , Eq. A1 may be written as

$$-n_i^2 I(\phi_i) = (Df_i)^0 - J(f_i^0, f_i^0) \quad (A26)$$

where

$$\begin{aligned} (Df)^0 = f^0 & \left\{ - \left[1 + \frac{2}{3} \left(\frac{m_i C_i^2}{2\theta_i} - \frac{3}{2} \right) [1 + 2(1 + e_i) g_{ii} \epsilon_i] \right. \right. \\ & + 2(e_i^2 - 1) g_{ii} \epsilon_i \left(\frac{m_i C_i^2}{2\theta_i} - \frac{3}{2} \right) \left. \right] \nabla \cdot \vec{v}_i + \vec{C}_i \cdot \left[\nabla \ln n_i \right. \\ & + \left(\frac{m_i C_i^2}{2\theta_i} - \frac{3}{2} \right) \nabla \ln \theta_i \left. \right] - \frac{1}{n_i} \nabla [n_i \theta_i + 2\theta_i n_i (1 + e_i) g_{ii} \epsilon_i] \cdot \frac{\vec{C}_i}{\theta_i} \\ & \left. + \frac{m_i}{\theta_i} \vec{C}_i \vec{C}_i : \nabla \vec{v}_i + \frac{2}{3} \left(\frac{m_i C_i^2}{2\theta_i} - \frac{3}{2} \right) \left[(e_i^2 - 1) g_{ii} \epsilon_i \frac{12}{d_i} \sqrt{\frac{\theta_i}{\pi m_i}} \right] \right\} \end{aligned} \quad (A27)$$

and

$$\begin{aligned} J_1(f^0, f^0) = -4\epsilon_i f^0 & \times \left\{ g_{ii} \left[2\vec{C}_i \cdot \nabla \ln n_i + \frac{(1 + e_i)^2}{4} \right. \right. \\ & \left. \left(\frac{3m_i C_i^2}{10\theta_i} - \frac{3}{2} \right) \vec{C}_i \cdot \nabla \ln \theta_i + \frac{m_i}{5\theta_i} (1 + e_i) \vec{C}_i \vec{C}_i : \nabla \vec{v}_i \right. \\ & \left. + \frac{3(1 + e_i)}{2} \left(\frac{m_i C_i^2}{5\theta_i} - 1 \right) \nabla \cdot \vec{v}_i \right. \left. + \vec{C}_i \cdot \nabla g_{ii} \right\} \end{aligned} \quad (A28)$$

After inserting the expression of each term in the right-hand side of Eq. A26, we obtain

$$\begin{aligned} -n_i^2 I(\phi_i) = f_0 & \left\{ \left[1 + \frac{3}{5} (1 + e_i)^2 g_{ii} \epsilon_i \right] \left(\frac{m_i C_i^2}{2\theta_i} - \frac{5}{2} \right) \vec{C}_i \cdot \nabla \ln \theta_i \right. \\ & + \left[1 + \frac{4}{5} (1 + e_i) g_{ii} \epsilon_i \right] \frac{m_i}{\theta_i} \left(\vec{C}_i \vec{C}_i - \frac{1}{3} C_i^2 \bar{I} \right) : \nabla \vec{v}_i \\ & + \frac{2}{3\theta_i n_i} \left(\frac{m_i C_i^2}{2\theta_i} - \frac{3}{2} \right) \left[(e_i^2 - 1) n_i \theta_i g_{ii} \epsilon_i \frac{12}{d_i} \sqrt{\frac{\theta_i}{\pi m_i}} \right] \\ & - 2(1 + e_i) g_{ii} \epsilon_i \vec{C}_i \cdot \nabla \ln \theta_i \\ & - 2 \left[1 - (e_i^2 - 1) g_{ii} \epsilon_i \left(\frac{m_i C_i^2}{2\theta_i} - \frac{5}{2} \right) \right] \vec{C}_i \cdot \nabla \cdot \vec{v}_i \\ & \left. + 4(1 - e_i) g_{ii} \epsilon_i \vec{C}_i \cdot \nabla \ln n_i + 2(1 - e_i) \epsilon_i \vec{C}_i \cdot \nabla g_{ii} \right\} \end{aligned} \quad (A29)$$

where ϕ_i is a sum of a linear combination of the components of $\nabla \ln \theta_i$, $\nabla \vec{v}$, and the scalar solution. Equating terms of the same tensorial order in Eq. A29, ϕ_i may be written as

$$\begin{aligned} \phi_i = -\frac{1}{n_i g_{ii}} & \{ F_i \cdot \nabla \ln \theta_i + G_i : \nabla \vec{v}_i - H_i \nabla \cdot \vec{v}_i \\ & + \alpha_{i1} + \vec{\alpha}_{i2} \cdot m_i + \alpha_{i3} m_i \} \end{aligned} \quad (A30)$$

$$F_i = \left(\frac{m_i}{2\theta_i} \right)^{1/2} \vec{C}_i \sum_{l=0}^q f_{i,l} S_{l/2}^l \left(\frac{m_i C_i^2}{2\theta_i} \right) \quad (A31)$$

$$G_i = \left(\frac{m_i}{2\theta_i} \right) \left(\vec{C}_i \vec{C}_i - \frac{1}{3} C_i^2 \bar{I} \right) \sum_{l=0}^{q-1} g_{i,l} S_{5/2}^l \left(\frac{m_i C_i^2}{2\theta_i} \right) \quad (A32)$$

$$H_i = \sum_{l=0}^{q-1} h_{i,l} S_0^l \left(\frac{m_i C_i^2}{2\theta_i} \right) \quad (A33)$$

with

$$S_k^q(x) = \sum_{j=0}^q \frac{\Gamma(k+q+1)}{(q-j)! j! \Gamma(k+j)} (-x)^j \quad (A34)$$

α_{i1} , α_{i2} , and α_{i3} are functions of r and t .

Following Chapman and Cowling,¹ α_{i1} , α_{i2} , and α_{i3} were chosen to satisfy

$$\int \psi f_i^0 \phi_i d\vec{c}_i = 0 \quad (A35)$$

where ψ_i is the property of any particle of phase i (that is, ψ_i may be mass, momentum, or energy).

It was found that the coefficients that satisfy Eq. A35 are

$$\alpha_{i1} = \alpha_{i2} = \alpha_{i3} = 0 \quad (\text{A36})$$

$$f_{i,0} = 8d_i\theta_i \sqrt{\frac{\pi}{m_i\theta_i}} \left[1 + \frac{3}{5} (1 + e_i)^2 g_{ii}\epsilon_i \right] / g_{ii} \quad (\text{A37})$$

$$g_{i,0} = 8d_i\theta_i \sqrt{\frac{\pi}{m_i\theta_i}} \left[1 + \frac{4}{5} (1 + e_i) g_{ii}\epsilon_i \right] / g_{ii} \quad (\text{A38})$$

$$h_{i,0} = 0 \quad (\text{A39})$$

Note that in the series Eqs. A31–A33 we retained only one term ($q = 1$, in the Sonine approximation).

Thus the expressions for the pressures and heat fluxes were obtained and can be written as follows:

First-Order Kinetic and Collisional Pressure Tensors

$$P_{ki}^1 = -\frac{5}{8d_i^2 g_{ii}} \left[1 + \frac{4}{5} (1 + e_i) g_{ii}\epsilon_i \right] \sqrt{\frac{m_i\theta_i}{\pi}} \dot{\nabla}^s \vec{v}_i \quad (\text{A40})$$

$$P_{cii}^1 = -\frac{5}{8d_i^2} \left[1 + \frac{4}{5} (1 + e_i) g_{ii}\epsilon_i \right] \frac{4(1 + e)\epsilon_i}{5} \sqrt{\frac{m_i\theta_i}{\pi}} \dot{\nabla}^s \vec{v}_i \quad (\text{A41})$$

First-Order Kinetic and Collisional Heat Fluxes

$$q_{ki}^1 = -\frac{75}{64d_i^2 g_{ii}} \left[1 + \frac{3}{5} (1 + e_i)^2 g_{ii}\epsilon_i \right] \sqrt{\frac{\theta_i}{m_i\pi}} \nabla \theta_i \quad (\text{A42})$$

$$q_{cii}^1 = -\frac{75}{64d_i^2} \frac{3}{5} (1 + e)^2 \epsilon_i \left[1 + \frac{3}{5} (1 + e_i)^2 g_{ii}\epsilon_i \right] \sqrt{\frac{\theta_i}{m_i\pi}} \nabla \theta_i \quad (\text{A43})$$

Manuscript received July 16, 2003, and revision received Oct. 15, 2004.